Available online at www.sciencedirect.com
SCIENCE DIRECT®
Journal of Molecular Catalysis A: Chemical 215 (2004) 169–175
JOURNAL OF MOLECULAR CATALYSIS A: CHEMICAL
www.elsevier.com/locate/molcata

Hydrothermally synthesized high silica mordenite as an efficient catalyst in alkylation reaction under liquid phase condition

Sujit Samanta [a], Nawal Kishor Mal [b], Prashant Kumar [c], Asim Bhaumik [a,*]

[a] *Department of Materials Science, Indian Association for the Cultivation of Science, Jadavpur, Kolkata 700032, India*
[b] *Dynamic Materials Research Group, National Institute of Advance Science & Technology (AIST), Osaka 563-8577, Japan*
[c] *Technical Chemistry & Heterogenous Catalysis, Aachen University, Aachen 52074, Germany*

Received 31 October 2003; received in revised form 20 January 2004; accepted 22 January 2004

Abstract

High silica mordenite (HSM) samples have been synthesized hydrothermally by using low aluminum contents (Si/Al molar ratios 40 and 60) with the synthesis gel in the presence of orthophosphoric acid as promoter at 443 K. Sodium silicate and aluminum sulfate were used as Si and Al precursors, respectively. Solid yield and particle size of these materials have been improved considerably over the conventional synthesis method for aluminous mordenite apart from high Si/Al molar ratios of the product and hydrothermal stability. These high silica mordenite samples showed excellent catalytic activity in the alkylation of benzene under liquid phase reaction conditions together with high selectivity towards linear alkyl benzenes. This catalytic performance suggested the presence of strong acid sites in this HSM material.

Keywords: High silica zeolite; Mordenite; Acid catalysis; Cracking; Linear alkyl benzene

1. Introduction

Zeolites with three-dimensional pores of molecular dimensions [1,2] have been used extensively as molecular sieves and catalysts in past three decades. A large number of synthetic zeolites with low Si/Al ratio have been synthesized, and several of them are used in acid catalyzed reactions, ion exchangers or sorbents [2]. The restricted geometry of pores and channel system in these materials are responsible for the shape-selective effect in the acid catalyzed reactions. Weak acidity of the acid sites along with poor thermal stability of these conventional Al-rich zeolites emphasized the need for the synthesis of the high silica [3] form of large pore zeolites to exploit their high acid strength. Mordenite (MOR) is an aluminous zeolite consisting of parallel 12-membered ring (MR) channels with dimensions of 6.5 Å × 7.0 Å that are interconnected by eight MR side pockets of 2.6 Å × 5.7 Å [4]. Strong acid sites in these zeolites are usually generated through steaming [5] or dealumination [6] processes since their hydrothermal synthesis in high silica form often leads to the contamination with undesired impurity phases like zeolite P, crystoballite, quartz, etc. [7]. The most renowned way to produce high silica mordenite is by post synthesis hydrothermal treatment in the presence of steam. The steaming is usually performed at very high temperature (above 723 K) on the ammonium (or hydrogen) form zeolite where hydrolysis of Al–O–Si bonds takes place. The aluminum is finally expelled from the framework causing a vacancy (hydroxyl nest) or partial amorphization of the framework. Si fills parts of the vacancies while others grow to form mesopores. On the other hand, dealumination required repeated post synthesis treatment of the aluminous zeolites for prolonged reaction time with mineral acids at elevated temperatures and long work-up process leading to a decrease in crystallinity of the zeolite. Although there are many reports on low Al containing mordenite [8], in most cases dealumination techniques have been used to increase the Si/Al ratio and this dealumination of H-MOR created intracrystalline mesopores [9], the volume of which increased with the degree of dealumination. In addition, dealumination removed the less acidic hydroxyls and hydroxyls became more acidic and more homogeneous. Another way to enhance acidity and Si/Al ratio is via post synthesis acid leaching with complexing agent like oxalic acid [10]. However, these methods

* Corresponding author. Tel.: +91-3324734971; fax: +91-3324732805.
E-mail address: msab@mahendra.iacs.res.in (A. Bhaumik).

1381-1169/$ – see front matter © 2004 Elsevier B.V. All rights reserved.
doi:10.1016/j.molcata.2004.01.017

usually lead to a loss of Si associated with loss of crystallinity of the material and thermal stability of the material. Further, mesoporosity is sometimes disadvantageous for shape selective catalysis. Thus, direct hydrothermal synthesis of catalytically active H-MOR [11] beyond Si/Al molar ratio of 6.0 in the synthesis gel devoid of other impurity phases is highly desirable. Specialized synthesis condition in the presence of template and mineralizer [12] have been reported recently to achieve Si/Al = 25 in high silica mordenite.

Linear alkylbenzenes (LABs) are important intermediates in detergent builders and these are largely produced industrially through alkylation of benzene with olefins using $AlCl_3$ or HF as catalyst [13]. Linear alkyl sulfonates (LAS) are extensively used worldwide as surfactant based biodegradable detergents and these are produced through the sulfonation of LABs. However, the lack of recycling and hazardous nature of the catalysts used for these reactions has emphasized the need for a suitable heterogeneous acid catalyst serving under mild and non-hazardous reaction conditions. In recent times this alkylation reaction have been found to be catalyzed efficiently in the presence of strong acid sites of high [14] and low silica [15] zeolites as well as immobilized ionic liquids [16]. Very recently UOP has reported the DETAL technology as a new alkylation process [17] for the alkylation of benzene with the heavy olefins, using solid acid as catalysts in the liquid phase reaction [18]. High silica MOR with strong acid sites can be a good catalyst for these alkylation reactions. Use of promoter oxianion [19] during the gel preparation in hydrothermal synthesis was known to enhance the crystallization rate and thus to improve the textural properties of zeolites. Herein, we report a promoter-based approach for the hydrothermal synthesis of catalytically active high silica mordenite (HSM) with high Si/Al ratios in the synthesis gels for the first time. These high silica mordenite samples showed good catalytic activity in alkylation of benzene using 1-dodecene in liquid phase with high selectivity for LABs.

2. Experimental

For the synthesis of high silica mordenite, sodium silicate (28% SiO_2, 30% Na_2O) was used as the silica source for all the syntheses. Hydrothermal synthesis was carried out with or without using orthophosphoric acid (85%, Loba Chemie) as promoter. In a typical synthesis, desired amount of sodium silicate solution was first diluted with water and then allowed to mix with an aqueous solution of aluminum sulfate with constant stirring for 15 min. White aluminosilicate gel was formed and the pH of the gel slowly increased. Then, the required amount of phosphoric acid dissolved in water and added onto this aged silica gel. When phosphoric acid was not used, equivalent amount of dilute aqueous HCl solution was added to maintain the pH. The final mixture was vigorously stirred for 1 h and then charged into an autoclave at 443 K for 5 days. pH of the gels were 11.2–11.8 in different hydrothermal batches. The molar ratio of constituents in the hydrothermal gels were:

$$SiO_2 : Al_2O_3 : H_3PO_4 : NaOH : H_2O = 1 : (0.0125 - 0.0083) : 0.15 : 1.04 : 25.$$

After the hydrothermal treatment, the solid products were filtered, washed with water and dried in air. For comparison, a conventional synthesis [7] of mordenite (low silica) was carried out using fumed silica as silica source at a synthesis temperature of 443 K for 1 day without the use of any promoter. The products were recovered by filtration and washing until pH dropped below 8.5. These materials were further evaluated and characterized by techniques such as XRD, N_2 sorption, SEM-EDS, FT-IR and solid state MAS NMR. All the samples were identified by powder XRD using a Shimadzu XRD-6000 diffractometer on which the small and wide-angle goniometers are mounted. The X-ray source was Cu Kα radiation ($\lambda = 0.15406$ nm) with a voltage and current of 40 kV and 30 mA, respectively. N_2 adsorption measurements were carried out using a BELSORP 28SA at 77 K. Prior to N_2 adsorption, samples were degassed for 2 h at 323 K. Morphology and particle size of the samples were analyzed using a Philips Xl-30/FEG, XL-serial scanning electron microscopy with an EDS (New XL-30) attachment. NMR experiments were carried out on a Bruker DSX500 machine equipped with a wide-bore super conducting magnet operating in a field-strength of 11.744 T. The base frequencies for ^{27}Al was 130.41 MHz and that for ^{29}Si was 99.43 MHz. Magic angle spinning (MAS) with a rotational speed of 5 kHz was applied for all the spectra and controlled with a MAS-control-unit (type H 2620, stability ± 2 Hz). The ^{29}Si NMR was referenced with respect to external TMS. All ^{27}Al chemical shifts were referred to external $[Al(H_2O)_6]^{3+}$ present in a saturated aqueous solution of $Al(NO_3)_3{\cdot}H_2O$. The data processing were performed with the Bruker X-WINNMR 2.5 software. A flow injection hydride generation unit attached to an atomic absorption spectrophotometer (Perkin-Elmer 2380 AAS) was used for wet chemical analysis. Prior to the chemical analysis solid samples were dissolved in minimum amount of concentrated HF and HCl solutions followed by evaporation for three times before making up the desired volume by distilled water.

For the preparation of H-form of the zeolites, initially 1 g of each of the solid Na-zeolites was taken in 100 ml of 1 M ammonium acetate solution in water and the resulting slurry was refluxed at 343 K for 4 h. After the exchange, the solid was washed with de-ionized water and dried under vacuum at room temperature. Heating of the exchanged solid sample at 723 K for 6 h to get the H-form of the zeolites followed this. Cumene cracking reactions were performed in an atmospheric pressure flow system. The catalyst that was placed in a quartz tube reactor 10 mm in diameter was first dehydrated at 673 K for 1 h in a nitrogen flow. The temperature was then brought into a desired reaction temperature

(523–623 K). The reactant was fed into the catalyst bed with a micro-feeder. Nitrogen was used as a career gas (flow rate 40 ml/min). The time factor (W/F = amounts of catalyst loaded divided by the flow rate of reactant gas) was 0.2 g h cc^{-1} and partial pressure of cumene was 7.9 kPa. The liquid phase alkylation of benzene was carried out in a two necked batch reactor placed in an oil bath at a constant temperature 353 K. Catalyst amount was 6 wt.% with respect to benzene and molar ratio of benzene/dodecene was 10:1. Reaction products were analyzed after 1h using a capillary gas chromatograph Agilent 4890D fitted with an FID detector.

3. Results and discussion

3.1. Synthesis

We have prepared high silica mordenite samples hydrothermally using a low concentration of Al in the synthesis gel and identified the nature of Si and Al species present in these high silica materials. Physico-chemical properties of various mordenite samples synthesized in the present study are presented in Table 1. It is pertinent to mention that unlike conventional synthesis of mordenite using fumed silica as silica source here for all the synthesis batches commercial grade sodium silicate were used. Although synthesis time have been prolonged for this Si precursor, yield of the final products have been improved drastically (Table 1). Particle sizes observed in these samples were also much smaller than those synthesized under conventional conditions.

3.2. Characterizations

In Fig. 1, XRD patterns of different high and low silica mordenite samples are shown. Sample 1 (Fig. 1a) was synthesized under conventional synthesis conditions without the addition of H_3PO_4 as a promoter [19] to the synthesis gel. XRD pattern of the high silica mordenite (samples 2) using the phosphate promoter is shown in Fig. 1b. Fig. 1c corresponds to sample 4. Except sample 4 all other samples (samples 1–3) were highly crystalline and show similar X-ray diffraction patterns to those of conventional mordenite [7]. The peak positions remained almost the same for samples 1–3, although little change in the intensity was observed. Wet chemical analysis indicated that with the increases in the Si/Al molar ratio of the gel from 40 to 60, an increase in the corresponding Si/Al ratio in the solid products was observed. Elemental analyses of various samples along with their corresponding surface areas are shown in Table 1. However, beyond Si/Al = 60 even in the presence of promoter-containing gel, impurity α-quartz phase start growing along with the mordenite phase. XRD pattern for sample 4 showed that apart from peaks characteristic of mordenite (pattern a and b), a competing α-quartz phase as well. Thus, materials obtained with the Si/Al molar ratio of 60 or less in the synthesis gel were crystalline high silica mordenite materials, whereas further decreasing the aluminum loading in the gel resulted in undesired products.

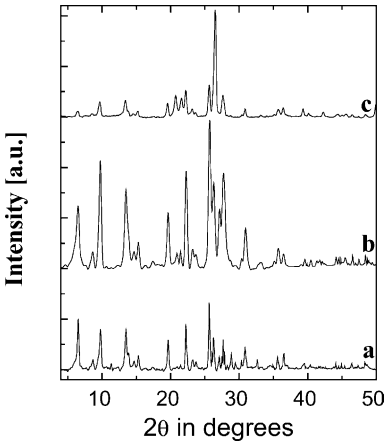

Fig. 1. XRD pattern of different mordenite samples 1 (a), 2 (b) and 4 (c).

In Fig. 2, the N_2 adsorption/desorption isotherms for high silica mordenite sample 2 (taken as representative) is shown. This isotherm was typically type I [20] in nature. At high P/P_0, some deviation from type I isotherm was observed for some other samples along with desorption hysteresis. This may be due to intracrystalline mesopores. The BET surface areas of mordenite samples were in the range 247–386 m^2 g^{-1}. FT-IR spectra of high silica mordenite samples showed a broad band in the hydroxyl region between 3700 and 3000 cm^{-1} with a maximum at ca.

Table 1
Synthesis condition and physico-chemical properties of different zeolite samples synthesized and used in the present study

Sample number	Zeolites	Synthesis time (d)	Synthesis temperature (K)	Yield[a]	Si/Al molar ratio		BET surface area (m2 g^{-1})
					Gel	Product	
1	Mordenite[b]	1.0	443	18.4	6.0	5.7	386
2	HSM	5.0	443	83.2	40.0	33.4	288
3	HSM	5.0	443	78.5	60.0	51.3	247
4	HSM + α-quartz	5.0	443	76.0	80	67.5	84
5	Al-MCM-41	1.0	373	95.8	15.0	18.0	987
6	$SiO_2/AlCl_3$	0.1	353	100.0	20.0	18.5	186

[a] Amount of solid product (g) obtained with respect to the total amount of SiO_2 and Al_2O_3 in gel.
[b] Fumed silica was used as silica source, other HSM samples were synthesized with sodium silicate.

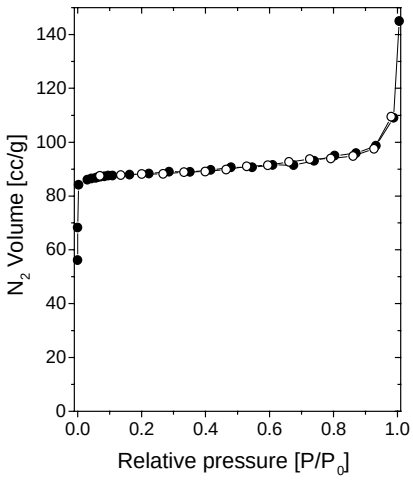

Fig. 2. N_2 adsorption/desorption isotherms of sample 2; adsorption points are marked with filled circle (●) whereas that for desorption points are with empty circles (○).

3450 cm^{-1}. This band can be assigned due to the framework SiO–H, as well as Si(OH)Al groups in interaction with the defect sites. SEM image of a representative high silica mordenite sample is shown in Fig. 3. Particles are quite small and composed of an aggregation of 1.5–1.8 μm long and 0.5–1 μm wide plate to rectangular crystallites. Al-rich mordenites are usually in the form of irregular needle, cylindrical or prismatic crystallites ∼1–15 μm in size.

^{27}Al and ^{29}Si MAS NMR studies have been carried out to examine the coordination and chemical environment around silicon in the HSM samples. The Si/Al ratio measured from the NMR data for sample 2 was 32.9 in agreement with that of 33.4 determined by wet chemical analysis. In Fig. 4 ^{27}Al MAS NMR spectrum of representative HSM sample 2 is shown. A strong signal with chemical shift at ∼55.4 ppm with respect to $[Al(H_2O)]^{3+}$ and no other downfield signal is a clear indication that almost all Al sites are tetrahedral.

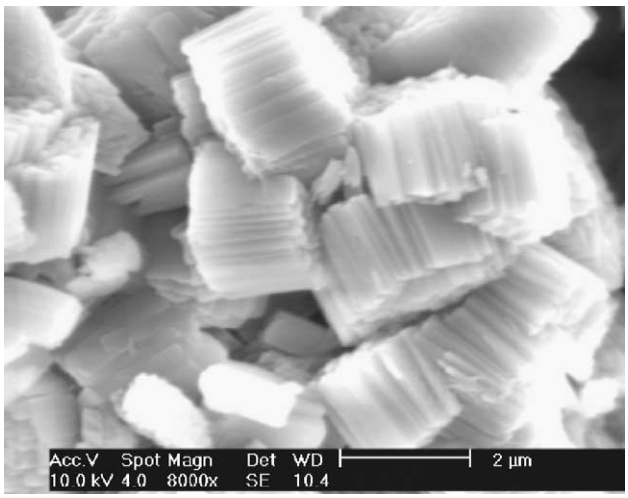

Fig. 3. SEM image of sample 2.

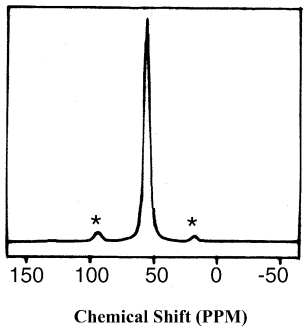

Fig. 4. ^{27}Al MAS NMR spectra of sample 2. Spinning side bands are marked with asterisk.

In Fig. 5, the ^{29}Si MAS NMR spectra of an HSM sample 2 (pattern a) is shown. The chemical shifts and their corresponding deconvoluted patterns (b–e) agree well with other aluminosilicate zeolites [2] or pure silica zeolite beta with no connectivity defect [21]. In aluminosilicates, replacement of one or more Si atoms in a Q^4 unit by Al atoms causes a significant paramagnetic shift. As seen in the figure for the deconvoluted data, four peaks were observed; the peaks between −114.4 and −107.6 ppm should all belong to Q^4 sites. Their chemical shift inequivalence was due to their occupancy in different crystallographic tetrahedral sites of the MOR framework. Similar observation was noticed for high silica zeolite beta [21]. In this low Al-containing zeolite, Q^3 peaks for Si(3Si, 1OH) was very minor and they tend to overlap with the resonances of Si(3Si, 1Al), appearing at ca. −100.9 ppm. Considering the high Si/Al ratio of sample 2, it is reasonable to assign the peak at −100.9 ppm to Si(3Si, 1OH) and /or Si(3Si, 1Al). Total area for the Q^4 sites were 92.6%, vis-à-vis Q^3 sites of 7.4%. The presence of Q^4 species in high concentration may support high degree of condensation among the silanol groups resulting in more cross-linkages and very little defect site concentrations.

3.3. Catalysis

Cumene cracking reactions were carried out in the gas phase over high (sample 2) and low silica (sample 1)

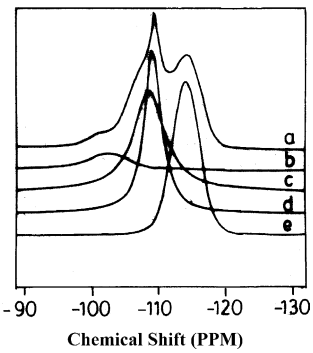

Fig. 5. ^{29}Si MAS NMR spectra of HSM sample 2 (a) and its deconvoluted patterns (b–e).

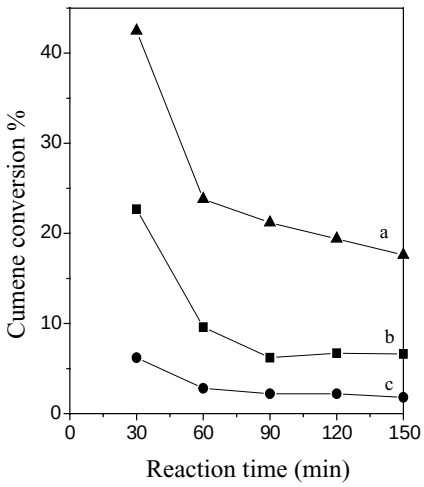

Fig. 6. Kinetic profile for cumene cracking over H-HSM (Si/Al = 33.4, a), Al-MCM-41 (Si/Al = 18.0, b), and H-MOR (Si/Al = 5.7, c).

mordenites as well as standard Al-MCM-41 (Si/Al = 18). Cumene conversion has been plotted against the reaction time in Fig. 6. From the figure, it is seen that for the high silica mordenite sample highest cumene conversion was observed. Al-rich sample 1 showed much lower activity and fast deactivation (plot c). Selectivity for aromatics was also high for the high silica mordenite sample (plot a). The higher cracking activity of this aluminum deficient high silica mordenite sample suggests that the acidic strength of Brönsted acid sites is much stronger than Al-rich mordenite and relatively stronger than mesoporous Al-MCM-41.

The alkylation of benzene with 1-dodecene was carried out in the liquid phase. Isomerization and alkylation reactions are known to be catalyzed by different solid acid catalysts [22–30]. Other catalysts, viz. HSM samples, SiO_2 (Degussa), MCM-41 (siliceous one), $AlCl_3$ supported on silica (Si/Al = 18.5), immobilized ionic liquid on MCM-41 and aluminus mordenite (sample 1) were also used for comparison. The ionic liquid used was made from aluminum chloride and 1-butyl-3-methylimidazolium chloride (2:3 molar composition). This ionic liquid is strongly acidic in nature and a good control catalyst for alkylation reaction [16]. Table 2 shows a comparison of the conversions and selectivities in the alkylation of benzene with dodecene catalyzed by these catalysts. The conversions were based on the concentrations

Table 2
A comparison of the conversions and selectivities in the alkylation of benzene with dodecene over different catalysts

Catalyst	Dodecene conversion (mol%)	Selectivities mole (%)		
		Dodecene isomers	Monoalkylated	Heavier
SiO_2	0.0	0.0	0.0	0.0
MCM-41	0.0	100.0	0.0	0.0
$SiO_2/AlCl_3$	18.0	80.0	20.0	0.0
MCM-41[a]	100.0	11.0	87.0	2.0
H-MOR (sample 1)	7.0	98.4	1.6	0.0
HSM (sample 2)	72.0	64.7	35.3	0.0
HSM (sample 3)	67.7	60.4	39.6	0.0

Reaction time = 1 h.
[a] Immobilized with ionic liquid.

of 1-dodecene alone. Thus, the isomerization of 1-dodecene was not considered as conversion, even though the different isomers of dodecene can alkylate the benzene molecule. This calculation method has been chosen since the isomerization reaction is an unwanted parallel reaction over the alkylation and can already be also catalyzed by weak acid sites. In the reactions catalyzed by the MCM-41 alone, the analysis of the reaction mixture showed no alkylation products. The low Brönsted acidity of the MCM-41 caused by silanol groups on the surface was not sufficient to catalyze the alkylation reaction. Nevertheless, a small amount of isomerization product was detected, while the reaction catalyzed by the amorphous silica showed no conversion at all. Immobilized ionic liquid supported on siliceous MCM-41 shows the complete conversion of dodecene [16] due to its highly Lewis acid character. From Table 2, it is seen that the dodecene conversions have been drastically improved in HSM samples over the conventional mordenite with low Si/Al. For sample 3 with low Al, total yield for the monoalkylated product was higher than that for sample 2.

Selectivity for a particular alkylated product is the most desirable in Friedel-Crafts alkylation reactions. A high conversion could be easily achieved with a strong acid catalyst, but the product range can vary strongly (Table 3). In the alkylation of benzene with dodecene, the desired product is the monoalkylated compound, in particular 2-phenyldodecane due to its easy biodegradability. Selectivity for this monoalkylated product was very high for

Table 3
Selectivity of the mono-alkylated products in alkylation over different catalysts and comparison with high silica mordenite[a]

Catalyst	Reaction temperature (K)	2-Phenyl-dodecene	3-Phenyl-dodecene	4-Phenyl-dodecene	5-Phenyl-dodecene	6-Phenyl-dodecene
H_2SO_4	273	20.0	17.0	16.0	23.0	24.0
$AlCl_3$	303	32.0	18.7	16.3	16.5	16.5
MCM-41[b] (6)	353	47.0	19.5	12.4	11.0	10.1
HSM (2)	353	61.9	24.7	12.4	0.0	1.0

[a] Selectivities in each case are the distribution for different isomers in the monoalkylated products.
[b] Immobilized ionic liquid.

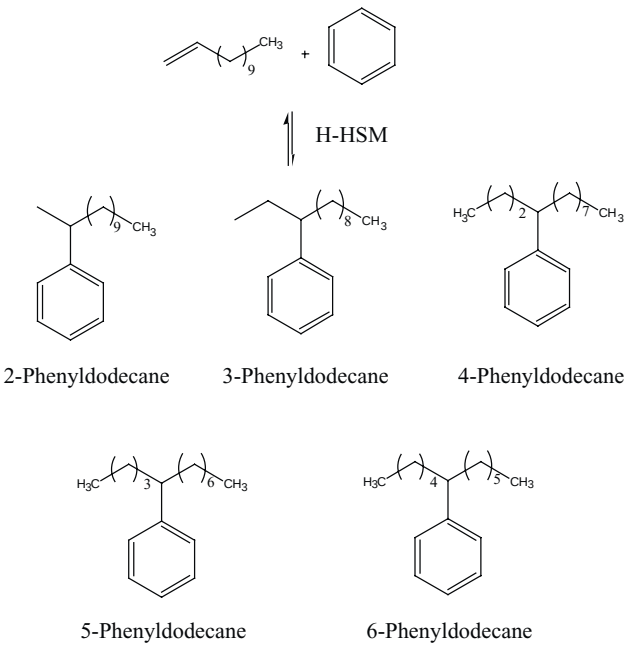

Fig. 7. Reaction scheme for alkylation of benzene.

sample 2 (Table 3). The other four different isomers of the monoalkylated product, 3-, 4-, 5- and 6-phenyl-dodecane, were also formed. Reaction schemes for all the desired products are shown in Fig. 7. The presence of different isomers is because of the shift in the intermediate carbenium ion, which could be formed in two steps, due to the interaction between the olefin and acid site of the catalyst followed by the attack of the benzene ring. The terminal product (1-phenyldodecane) was not formed since the reaction follows the Markovnikov rule (least stability of the primary carbenium ion). Effect of the different catalysts in the distribution of monoalkylated isomers is illustrated in Table 3. The selectivity for the reactions could be explained by the ability of solid acid to isomerize the phenylalkane formed. The distribution of isomers found for the reaction catalyzed by high silica mordenite samples showed moderately higher amount of 2-phenyldodecane compared to other catalysts.

4. Conclusions

We have synthesized high silica mordenite hydrothermally with high Si/Al molar ratios up to 60 (51.3 in the product) in the synthesis gel in the presence of H_3PO_4 promoter and sodium silicate as Si precursor. Although the synthesis time was prolonged, the yield has been improved and small plate like crystals of HSM materials were formed. FT-IR spectroscopic studies and cumene cracking reactions showed high acidity of these high silica mordenite samples over the well-known low silica mordenite. Excellent catalytic activity in the alkylation of benzene under liquid phase reaction conditions together with high selectivity towards 2-phenyldodecane isomer indicated strong acid sites in these HSM materials. Strong acid sites in these promoter-induced hydrothermally synthesized H-HSM materials suggest an easy and alternative pathway for the synthesis of high silica mordenite prevailing over the existing steaming and dealumination processes.

Acknowledgements

AB wishes to thank DST and CSIR, New Delhi, for the financial help.

References

[1] R.M. Barrer, Hydrothermal Chemistry of Zeolites, Academic Press, New York, 1982.
[2] R. Szostak, Molecular Sieves: Principles of Synthesis and Identification, Van Nostrand Reinhold, New York, 1989.
[3] M.I. Levinbuk, M.L. Pavlov, L.M. Kustov, J.P. Fraissard, T.V. Vasina, A.V. Kazakov, Y.I. Azimova, Y.Y. Smorodinskaya, Appl. Catal. A 172 (1998) 177.
[4] N. Katada, Y. Kageyama, M. Niwa, J. Phys. Chem. B. 104 (2000) 7561.
[5] K.-H. Lee, B.-H. Ha, Microporous Mesoporous Mater. 23 (1998) 211.
[6] M. Müller, G. Harvey, R. Prins, Microporous Mesoporous Mater. 34 (2000) 135.
[7] G.J. Kim, W.S. Ahn, Zeolites 11 (1991) 745.
[8] B.L. Meyers, T.H. Fleisch, G.J. Ray, J.T. Miller, J.B. Hall, J. Catal. 110 (1988) 82.
[9] M. Tromp, J.A. van Bokhoven, M.T. Garriga Oostenbrink, J.H. Bitter, K.P. de Jong, D.C. Koningsberger, J. Catal. 190 (2000) 209.
[10] R. Giudici, H.W. Kouwenhoven, R. Prins, Appl. Catal. A 203 (2000) 101.
[11] K. Segawa, S. Mizuno, M. Sugiura, S. Nakata, Stud. Surf. Sci. Catal. 101 (1996) 267.
[12] H. Sasaki, Y. Oumi, K. Itabashi, B. Lu, T. Teranishi, T. Sano, J. Mater. Chem. 1173 (2003).
[13] Ulllmann's Encyclopedia of Industrial Chemistry, J.E. Bailey et al. (Eds.), sixth ed., Wiley-VCH, 2001.
[14] L.B. Young, US Patent 4,301,317, 1981.
[15] B.L. Su, D. Barthomeuf, Appl. Catal. A 124 (1995) 81.
[16] C. DeCastro, E. Sauvage, M.H. Valkenburg, W.F. Hoelderich, J. Catal. 196 (2000) 86.
[17] C.J. Adams, M.J. Earle, G. Roberts, K.R. Seddon, Chem. Commun. (1998) 2097.
[18] K. Tanabe, W.F. Hoelderich, Appl. Catal. A: Gen. 181 (1999) 399.
[19] R. Kumar, A. Bhaumik, R.K. Ahedi, S. Ganapathy, Nature 381 (1996) 298.
[20] S.J. Gregg, K.S.W. Sing, Adsorption, Surface Area and Porosity, Academic, London, 1982.
[21] M.A. Camblor, A. Corma, S. Valencia, Chem. Commun. (1996) 2365.
[22] J.-H. Kim, T. Matsuzaki, K. Takeuchi, T. Hanaoka, Y. Kubota, Y. Sugi, X. Tu, M. Matsumoto, Adv. Mater. 93 (1994) 153.
[23] M. Guisnet, P. Ayrault, J. Datka, Pol. J. Chem. 71 (1997) 1455.
[24] L.D. Fernandes, J.L.F. Monteiro, E.F. Sousa-Aguiar, A. Martinez, A. Corma, J. Catal. 177 (1998) 363.
[25] M.D. Macedonia, D.D. Moore, E.J. Maginn, M.M. Olken, Langmuir 16 (2000) 3823.
[26] F.J.J.M. De Gauw, J. van Grondelle, R.V. van Santen, J. Catal. 204 (2001) 53.

[27] G. Tasi, F. Mizukami, I. Pálinkó, M. Toba, A. Kukovecz, J. Phys. Chem. A 105 (2001) 6513.
[28] A.M. Vos, X. Rozanska, R.A. Schoonheydt, R.A. van Santen, F. Hutschka, J. Hafner, J. Am. Chem. Soc. 123 (2001) 2799.
[29] Z.-M. Wang, T. Arai, M. Kumagai, Ind. Eng. Chem. Res. 40 (2001) 1864.
[30] I.I. Ivanova, V. Montouillout, C. Fernandez, O. Marie, J.P. Gilson, Microporous Mesoporous Mater. 57 (2003) 297.